Received: 15 August 2023 | Revised: 9 October 2023 | Accepted: 10 November 2023

DOI: 10.1111/sji.13341

Scandinavian Journal of Immunology An International Monthly Journal WILEY

ORIGINAL ARTICLE

Identifying a core protein signature of small extracellular vesicles derived from B-cell precursor acute lymphoblastic leukaemia

Nathaniel Edward Bennett Saidu[1] | **Miriam Aarsund**[1] | **Eva Sørensen**[2] | **Maria Stensland**[3] | **Tuula Anneli Nyman**[3] | **Aina Ulvmoen**[4] | **Yunjie Wu**[1] | **Marit Inngjerdingen**[1]

[1]Department of Pharmacology, Institute of Clinical Medicine, University of Oslo, Oslo, Norway

[2]Department of Biosciences, University of Oslo, Oslo, Norway

[3]Department of Immunology, University of Oslo and Oslo University Hospital, Oslo, Norway

[4]Department of Pediatrics, Oslo University Hospital, Oslo, Norway

Correspondence
Marit Inngjerdingen, Department of pharmacology, Sognsvannsveien 20, 0372 Oslo, Norway.
Email: mariti@medisin.uio.no

Present address
Nathaniel Edward Bennett Saidu, Department of Cancer Immunology, Institute of Cancer Research, Oslo University Hospital, Oslo, Norway

Funding information
Barnestiftelsen at Oslo Universitetssykehus; Fondsstiftelsen at Oslo Universitetssykehus; The South-Eastern Regional Health Authority; UNIFOR-FRIMED

Abstract

Acute paediatric leukaemia is diagnosed and monitored via bone marrow aspirate assessment of blasts as a measure of minimal residual disease. Liquid biopsies in the form of blood samples could greatly reduce the need for invasive bone marrow aspirations, but there are currently no blood markers that match the sensitivity of bone marrow diagnostics. Circulating extracellular vesicles (EVs) represent candidate biomarkers that may reflect the blast burden in bone marrow, and several studies have reported on the utility of EVs as biomarkers for adult haematological malignancies. Increased levels of EVs have been reported for several haematological malignancies, and we similarly report here elevated EV concentrations in plasma from paediatric BCP-ALL patients. Plasma EVs are very heterogeneous in terms of their cellular origin, thus identifying a cancer selective EV-marker is challenging. Here, we undertook a reductionistic approach to identify protein markers selectively associated to plasma EVs derived from BCP-ALL patients. The EV proteome of primary BCP-ALL cell-derived EVs were compared against EVs from healthy donor B cells and the BCP-ALL cell line REH, and further against EVs isolated from plasma of healthy paediatric donors and paediatric BCP-ALL patients. With this approach, we identified a signature of 6 proteins (CD317, CD38, IGF2BP1, PCNA, CSDE1, and GPR116) that were specifically identified in BCP-ALL derived EVs only and not in healthy control EVs, and that could be exploited as diagnostic biomarkers.

1 | INTRODUCTION

B-cell precursor acute lymphoblastic leukaemia (BCP-ALL) is an aggressive malignancy of immature B-lineage progenitors. The leukaemic cells arise in the bone marrow (BM) and infiltrate the liver, spleen and lymph nodes, and can spread further to the central nervous system. BCP-ALL is primarily a paediatric disease, and is the most common

form of acute leukaemia in children. With current treatment protocols, the 5-year overall survival is above 90%.[1] Patients are treated according to risk-adapted chemotherapy treatment protocols, with more intense treatment of high-risk patients. Initial risk status scoring is a powerful indicator of overall survival, and patients are categorized as non-risk or high-risk at diagnosis based on initial white blood cell counts and cytogenetics, with further stratification after induction therapy on day 29. The gold standard for measuring treatment response in paediatric leukaemia is by BM aspiration aimed at detecting minimal residual disease, by combining real-time quantitative PCR and cytology. Ideally, a less invasive diagnostic blood test could spare patients anaesthetic procedures necessary for bone marrow aspiration. In this context, BCP-ALL-derived extracellular vesicles (EVs) could represent a putative biomarker for monitoring of the leukaemia.

EVs are released from all cells, and function as carriers of macromolecules between cells, and can thereby modify the function of the receiving cell. EVs show considerable heterogeneity of size and cargo that is dependent on their origin. They may derive from the plasma membrane in the form of microparticles, or from the endosomal compartment in the form of exosomes.[2] Cancer cells may also release larger vesicles, oncosomes, which are released as a result of blebbing from the cancerous cells. Multiple studies have demonstrated that EVs released from cancer cells carry mRNA, microRNA and proteins that interact with and functionally affect receiving cells.[3,4] Tumour-derived EVs can promote increased malignancy,[5] metabolically re-program target cells, and support tumour growth and metastasis by shaping of the tumour microenvironment.[6–8] Specifically, BCP-ALL oncosomes are suggested to promote blast infiltration into the central nervous system.[9] Detection of tumour-derived EVs in blood or other body fluids may serve as useful biomarkers to diagnose and monitor disease progression.[10,11] For haematological cancers, increased concentrations of plasma EVs have been detected in acute myeloid leukaemia (AML) and ALL patients.[12,13] EVs carry a signature reflected by their parental cells, and with respect to B cells, B-cell-derived EVs are shown to carry B-cell markers such as CD19 and CD20.[14]

Although plasma serves as a practical source for diagnostic purposes, plasma EVs are highly heterogenous, with EVs originating from several different cellular sources including platelets, endothelial cells and leukocytes. To precisely identify cancer-derived EVs it is necessary to identify and employ a cancer cell specific marker. This study aimed at identifying a BCP-ALL-specific protein signature in plasma EVs derived from BCP-ALL patients, to instruct future biomarker designs for use in risk stratification, disease monitoring, and prediction of treatment response.

2 | MATERIALS AND METHODS

2.1 | Patients and healthy controls

Peripheral venous blood (5 mL) with heparin as anticoagulant was collected from paediatric BCP-ALL patients ($n = 14$) (Table 1) admitted between January 2014 and November 2017 at Oslo University Hospital, Oslo, Norway during routine diagnostic procedures. Peripheral venous blood was also collected with heparin as anticoagulant from healthy age-matched children ($n = 18$) undergoing elective procedures at Oslo University Hospital in the period January 2014 – April 2018. Plasma was stored at −80°C until use. All samples were obtained after informed, written parental consent according to the Declaration of Helsinki and the study was approved by the South-Eastern Norway Regional Ethical Committee (REK2013/1866). Patients were treated according to the risk-adapted NOPHO (Nordic Society of Paediatric Haematology and Oncology) – ALL 2008 protocol [14]. ALL patients are initially grouped as non-high risk or high risk at diagnosis based on white blood cell count in blood and BM blast immunophenotype (B or T cell), and further grouped into standard, intermediate, or high risk based on BM cytogenetics and minimal residual disease (MRD) after induction therapy on day 29 [15]. In addition, blood samples were collected during induction therapy on days 15 and 29, after consolidation at day 79, and at the end of treatment. Buffy coats for separation of PBMCs from healthy adult volunteers were obtained

TABLE 1 Characteristics of patients and paediatric controls.

	Healthy paediatric controls	BCP-ALL patients
Numbers, *n*	18	14
Age at diagnosis, median (range)	7.0 (1–16)	4.0 (1–16)
WBC (10^9/L), median (range)		7.9 (0.9–167)
Cytogenetics		
SR		3/14
IR[a]		2/14
ETV6/RUNX1		6/14
Trisomy 21		1/14
Others (incl. CN)		3/14

Abbreviations: CN, cytogenetics negative; IR, intermediate risk; SR, standard risk; WBC, white blood cells.

[a]Intermediate risk cytogenetics: dic(9;20), *t*(1;19), Ic21amp = AML1.

from the blood bank at Oslo University Hospital according to the Declaration of Helsinki.

2.2 | Isolation of EVs from plasma

Plasma from BCP-ALL patients or paediatric healthy controls was collected within 6 h of sampling. The plasma was collected by separating away the red blood cells and white blood cells by gravity, followed by a spin at 2000 *g* for 15 min, thereafter a spin at 10 000 *g* for 20 min, filtering through 0.22 μm filters, and frozen at −80°C. Total plasma EVs were isolated from 1 mL of plasma via either the Total Exosome Isolation kit for plasma (ThermoFisher) or ExoSpin™ that combines precipitation and size-exclusion chromatography (Cell Guidance Systems) according to the manufacturer's instructions. EV pellets were resuspended in 50 μL PBS and stored at −80°C. For proteomic analysis, plasma EVs were purified via a two-step procedure by precipitation using the Total Exosome Isolation kit for plasma (ThermoFisher), followed by washing in PBS and ultracentrifugation at 180 000 *g* (average) for 2 h 15 min using the SW41Ti rotor.

2.3 | Isolation of small EVs from BCP-ALL blasts and primary B cells

Primary B cells from paediatric BCP-ALL patients or healthy adult donors were positively selected from frozen PBMCs using MACS CD19 MicroBeads (Miltenyi Biotech) per manufacturer's instruction. $1–3\times10^6$ purified B cells (more than 90% live) were cultured for 48 h in serum-free AIM-V medium in the presence of 100 ng/mL MegaCD40L (ThermoFisher Scientific), 10 ng/mL Flt3L, 10 ng/mL IL-7, and 10 ng/mL IL-3 at 1×10^6 cells/mL. Supernatants were spun at 400 *g* for 10 min, followed by 2000 *g* for 30 min to remove cells and cell debris. EVs were isolated by precipitation using the Total Exosome Isolation kit (ThermoFisher Scientific) according to the manufacturer's instructions, followed by washing in PBS and ultracentrifugation at 180 000 *g* (average) for 2 h 15 min using the SW41Ti rotor. The resulting EV pellets were resuspended in 50 μL PBS and stored at −80°C.

2.4 | Isolation of EVs from REH cells

The BCP-ALL cell line REH was cultured in complete RPMI (RPMI-1640 supplemented with 10% FBS, 1% penicillin/streptomycin, 1% sodium pyruvate, and 50 mM 2-mercaptoethanol), and split every 2 days. To produce EVs, REH cells were cultured at 2×10^6 cells/mL in serum-free AIM-V medium for 48 h, and supernatants spun at 400 *g* for 10 min followed by 2000 *g* for 30 min. EVs from 4 mL of REH supernatants were isolated using 5 different approaches in order to test optimal purification, (i) concentration through Amicon Ultra-4 centrifugal filters of 100 kDa cut-off (Merck) at 3000 *g* for 20 min, (ii) concentration through Amicon Ultra-4 centrifugal filters of 100 kDa cut-off (Merck) at 3000 *g* for 20 min followed by resuspending in 4 mL particle-free PBS and ultracentrifugation at 180 000 *g* (average) for 2 h 15 min using the SW41Ti rotor, (iii) precipitation using the Total Exosome Isolation kit (ThermoFisher) according to the manufacturer's instructions, (iv) precipitation using the Total Exosome Isolation kit (ThermoFisher) followed by resuspension in 4 mL particle-free PBS and ultracentrifugation at 180 000 *g* (average) for 2 h 15 min using the SW41Ti rotor, or (v) ultracentrifugation alone at 180 000 *g* (average) for 2 h 15 min using the SW41Ti rotor alone. The resulting EV pellets were resuspended in 50 μL particle-free PBS.

2.5 | Transmission electron microscopy.

EVs were imaged by negative stain electron microscopy. A 400 mesh copper grid with carbon-coated formvar film were placed on 20 μL EVs and incubated for 10 min. The grid was washed twice in water, excess liquid removed, and transferred to a drop of 2% uranyl acetate for 30 s, dried and subjected to microscopy with a Tecnai G^2 Spirit TEM (FEI) equipped with a Morada digital camera and RADIUS imagining software.

2.6 | Nanoparticle tracking analysis (NTA)

EVs were analysed using a LM10 nanoparticle tracking analyser with a 532-nm laser (Malvern Panalytics). In brief, 10 μL of EV isolates was diluted 1:1000 in sterile PBS and pumped through a 10 mL syringe that was attached to the nanoparticle tracking analyser. Nanoparticles were recorded in a total of 3 videos of 30 s for each sample and analysed under constant settings to obtain data on mean particle size, size distribution, and particle concentration. As NTA is most accurate between particle concentrations in the range of 2×10^8 to 2×10^9/mL, samples with higher counts were further diluted and re-analysed and the relative concentration calculated according to the distribution factor.

2.7 | Western blotting

EVs were lysed with 10 μL of lysis buffer (50 mM Tris–HCl, pH 8.0, 150 mM NaCl, 1% Triton X-100, protease

inhibitor cocktail Complete™ [Roche]) on ice for 15 min. The protein content of the lysate was determined using BCA Protein Assay Kit (ThermoFisher Scientific). Equal concentrations of EV proteins were separated on 12% Criterion SDS-PAGE gels (Bio-Rad) and transferred onto PVDF membranes (Merck Millipore). The membranes were blocked with 5% dry milk in TBS containing 0.5% Tween-20 (TBS-T) for 1 h at room temperature, and further blotted with either anti-CD63 (1:500; ThermoFisher Scientific), anti-CD81 (1:500; ThermoFisher Scientific), anti-IGF2BP1 (1:1000; ThermoFisher Scientific) and anti-PCNA (1:1000; ThermoFisher Scientific) as indicated in TBS-T containing 1% dry milk. Blots were probed with goat anti-rabbit IgG-HRP or goat anti-mouse IgG-HRP (Bio-Rad), and developed by Pierce ECL Western Blotting Substrate (ThermoFisher Scientific).

2.8 | Mass spectrometry analysis (LC–MS/MS)

EVs in PBS were subjected to LC–MS/MS analysis. Briefly, EVs were lysed by heating at 95°C for 20 min in 0.1% ProteaseMax Surphactant (Promega), followed by brief vortexing. A volume corresponding to 4 μg of proteins were reduced in 20 mM DTT for 30 min at 56°C and alkylated by addition of iodoacetamine to a final concentration 30 mM and incubation in the dark for 20 min at room temperature. Proteins were digested with 0.5 μg trypsin at 37°C overnight, and peptides were captured, concentrated, and desalted using C18 stage tips (Affinisep).

Samples were then analysed by a nanoElute UHPLC coupled to a timsTOFfleX mass spectrometer (Bruker Daltonics) via a CaptiveSpray ion source and a 25 cm reversed-phase C18 column (1.6 μm bead size, 120 Å pore size, 75 μm inner diameter, Ion Optics). A flow rate of 0.3 μL/min and a solvent gradient from 0% to 35% B in 60 min was used to separate the peptides. Solvent B was 100% acetonitrile in 0.1% formic acid and solvent A 0.1% formic acid in water. The mass spectrometer was operated in data-dependent Parallel Accumulation-Serial Fragmentation (PASEF) mode. Mass spectra for MS and MS/MS scans were recorded between m/z 100 and 1700. Ion mobility resolution was set to 0.60–1.60 V·s/cm over a ramp time of 100 ms. Data-dependent acquisition was performed using 10 PASEF MS/MS scans per cycle with a near 100% duty cycle. 10 PASEF MS/MS scans per cycle with a near 100% duty cycle. A polygon filter was applied in the m/z and ion mobility space to exclude low m/z, singly charged ions from PASEF precursor selection. An active exclusion time of 0.4 min was applied to precursors that reached 20 000 intensity units. Collisional energy was ramped stepwise as a function of ion mobility.

MS raw files were submitted to MaxQuant software version 2.0.1.0 for protein identification [35]. Parameters were set as follow: carbamidomethylation as fixed modification; protein N-acetylation and methionine oxidation as variable modifications. First search error window of 20 ppm and mains search error of 6 ppm. Trypsin without proline restriction enzyme option was used with two allowed miscleavages. Minimal unique peptides were set to 1, and FDR allowed was 0.01 (1%) for peptide and protein identification. Data analysis and visualization were done using FunRich version 3.1.4, InteractiVenn[15] and GraphPad Prism 9. The mass spectrometry proteomics data have been deposited to the ProteomeXchange Consortium via the PRIDE partner repository with the dataset identifier PXD044465.

2.9 | Statistics

The data were analysed using Graph Pad Prism and Perseus. Data depicted in graphs are presented as the mean standard error of the mean (SEM). Comparisons within an experimental group of data were performed using non-parametrical Mann–Whitney *U* test. *P* values less than .05 were considered statistically significant.

3 | RESULTS

3.1 | Increased EV abundance in plasma at diagnosis

The concentration of EVs in plasma was retrospectively tested in a cohort of 14 BCP-ALL patients (Table 1) at diagnosis, and compared against 18 healthy paediatric controls. The EVs were enriched via precipitation using the ThermoFisher Total Exosome Isolation kit or via Exo-Spin. We found increased particle concentrations in patients as assessed by NTA with both separation methods (Figure 1A). The particle size appeared similar between controls and patients with a median of app. 150 nm (Figure 1B). The protein concentration of the EV isolates was also higher in the EV isolates from BCP-ALL patients compared with controls, indicative of more EVs in the samples (Figure 1C). EM images confirmed the presence of vesicles with cup-shaped morphology (Figure 1D), but it was clear that the EV isolates contain a large amount of similarly-sized lipoprotein particles (white arrows) that confound a precise assessment of the EV concentration. The NTA particle counts made in Figure 1A,B thus also include lipoproteins and other protein complexes. Western blotting analysis of similar input of protein, showed presence of small EV-markers CD63, CD81 and Alix within the isolates, and absence of Cytochrome C (Figure 1E). The signals were stronger for

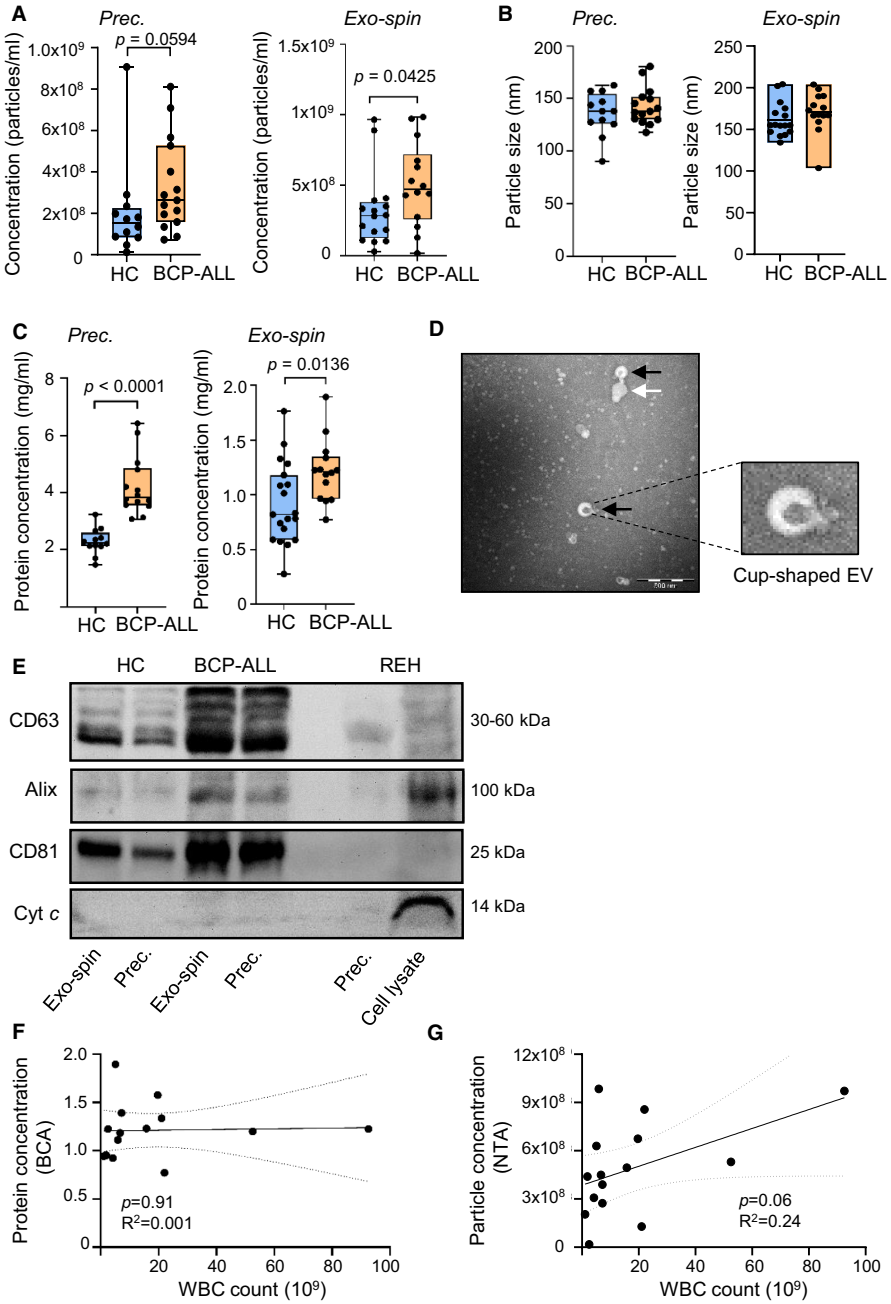

FIGURE 1 Increased EV concentration in BCP-ALL patients at diagnosis. Plasma EVs were isolated from 1 mL of plasma from BCP-ALL patients or healthy paediatric donors via either Total Exosome precipitation reagent or Exo-Spin™ columns. (A) Particle concentration was measured by NTA (precipitation: BCP-ALL ($n = 14$), healthy controls ($n = 12$); Exo-spin: BCP-ALL ($n = 14$), healthy controls ($n = 16$). (B) Mean particle size was measured by NTA (precipitation: BCP-ALL ($n = 14$), healthy controls ($n = 12$); Exo-spin: BCP-ALL ($n = 14$), healthy controls ($n = 16$). (C) Protein concentration of EV isolates was measured by BCA (precipitation: BCP-ALL ($n = 14$), healthy controls ($n = 18$); Exo-spin: BCP-ALL ($n = 12$), healthy controls ($n = 16$). (D) Electron microscopy image of one BCP-ALL EV sample. Scale bare 500 nm. The white arrow indicates a chylomicron, while the black arrow indicates an EV. (E) Western blot analysis of CD63, CD81, Alix, and cytochrome C from equal protein input of EV isolates from plasma of healthy controls or patients, isolated via either precipitation or Exo-Spin™. EVs from REH cells and REH cell whole cell lysate served as controls. HC, healthy control. Statistical significance was calculated using the non-parametrical Mann–Whitney test. (F) Correlation analysis of protein concentration or (G) particle concentration with white blood cell count (WBC).

samples derived from the patients, indicating that there indeed are more EVs in circulation at diagnosis. We next evaluated the utility of monitoring EV concentration as a diagnostic marker per se for BCP-ALL. However, we show that there is little correlation between WBC counts and particle concentration at diagnosis (Figure 1F,G). There was also no correlation between particle concentration and risk status or cytogenetics (data not shown). Measuring particle concentration at different timepoints throughout the induction period showed varying results and no correlation to treatment outcome or risk status (data not shown). We therefore conclude that a marker specific for BCP-ALL EVs must be identified to unleash the potential for EVs as a prognostic tool in this disease.

3.2 | Characterization of EVs from plasma and BCP-ALL blasts

In order to identify a BCP-ALL specific EV protein signature to help identify BCP-ALL-derived EVs in plasma, we undertook a reductionistic approach by comparing the proteome of plasma EVs with EVs derived from purified B cells from either healthy donors or patients.

As starting material was limited for the paediatric patients, we first optimized protocols for purification of EVs from low amounts of cells (<3 million) in order to maximize the number of identifications in LC–MS/MS-analysis. Forty-eight-hour serum-free culture supernatants from the REH BCP-ALL cell line were either (i) ultracentrifuged,

(ii) concentrated through a 100 kD filter, (iii) concentrated through 100 kD filters followed by ultracentrifugation, (iv) precipitated, or (v) precipitated followed by ultracentrifugation. While protocols omitting ultracentrifugation resulted in higher protein yields, it was clear that ultracentrifugation was necessary to reduce albumin contamination, which highly impacted on the number of identifications (Table S1 and Figure S1). With precipitation alone, more than 80% of the signal originated from albumin, in contrast to under 30% with protocols involving ultracentrifugation.

Subsequently, EVs were harvested from serum-free cytokine-supplemented 48 h-cultures of B cells purified from 3 healthy adult donors or from 2 standard risk BCP-ALL patients. We also isolated EVs from plasma of three healthy, paediatric controls and three BCP-ALL patients. For all samples, EVs were isolated via a two-step procedure of precipitation followed by ultracentrifugation. Samples were subjected to quantitative LC–MS/MS with equal protein concentration as input. Despite low input due to limited material and extensive purification protocols, we were able to detect a total 1882 proteins across the samples (an average 600 proteins in control plasma EVs, 717 proteins in BCP-ALL plasma EVs, 1188 proteins in healthy donor B-cell EVs and 1479 proteins in patient B-cell EVs, Table S2). A broad range of EV-markers were identified in the four sample sets, albeit sparser in EVs isolated from plasma (Figure 2A). The EV-marker set was based on a recent paper by Kugeratski et al.[16]

PCA analysis indicated that plasma EVs from BCP-ALL patients cluster together with plasma EVs from healthy controls, and are distinct from EVs directly derived from BCP-ALL or healthy B cells (Figure 2B). Gene set enrichment analysis indicated enrichment of proteins involved in metabolism within the EVs derived from the B cells of BCP-ALL patients (Figure 2C). We further show comparable expression of a panel of B-cell markers and HLA molecules by B-cell-derived EVs from both healthy donors and BCP-ALL patients (Figure 2D). Identified proteins were again sparser within plasma EVs, and apart from HLA molecules, B-cell markers were either not detected or present at very low levels in both healthy controls and patients. This underscores the difficulty of identifying B-cell-specific markers in plasma EVs in limited amount of starting material.

3.3 | Identification of a BCP-ALL specific EV signature

A direct comparison of the proteomic profile of all EV samples, including REH EVs, revealed a common core proteome of 403 proteins that include proteins commonly detected in EVs (Figure 3A and Table S2). By performing a 5-way Venn diagram analysis, we could identify four markers; CD38, Bone Marrow Stromal Cell Antigen 2 (BST2/CD317), Insulin-like growth factor 2 mRNA-binding protein 1 (IGF2BP1), and Proliferating Cell Nuclear Antigen (PCNA) to be uniquely present in REH cell EVs, BCP-ALL cell-derived EVs and BCP-ALL plasma EVs, but not in B-cell-derived EVs or plasma EVs from healthy controls (Figure 3A). Further, Cold Shock Domain-containing Protein E1 (CSDE1) and G-protein Coupled Receptor (GPR116) were only detected in EVs derived from BCP-ALL patients. To verify these findings, we tested the expression of IGF2BP1 and PCNA by Western blotting in 6 healthy controls and 8 patients, and show that these markers were expressed at higher levels in EVs from the patients (Figure 3B,C).

4 | DISCUSSION

In this study, we have utilized proteomics analysis as an approach to identify a core protein signature of EVs derived from BCP-ALL cells that is detectable in the plasma.

Release of large extracellular $CD19^+$ oncosomes from BCP-ALL blasts was previously demonstrated in bone marrow aspirates,[17] but small EVs has to our knowledge not previously been investigated for BCP-ALL. As has been reported for myeloid acute leukaemia, we show increased levels of EVs at diagnosis in BCP-ALL patients compared with controls. This was measured both as protein concentration of EV isolates and particle counts by NTA. We found that the results were comparable between the two EV isolation protocols utilized, but that there as expected was overall lower protein yields with the Exo-Spin protocol. The EV isolates had a median size around 150 nm in both patients and controls, confirming the isolation of small EVs, although we expect that lipoprotein particles and protein complexes contribute to the overall measurements by NTA.

Previous studies in AML have reported a correlation of blast load with EV abundance,[18] but we did not find any correlation between plasma particle concentration and white blood cell counts. This could reflect that other cells besides the blasts may also be contributing to the rise in EVs. Plasma EVs is a very heterogeneous population, representing EVs derived from platelets, endothelial cells, leukocytes and other cells releasing EVs into the circulation. In a study on paediatric ALL, the high level in plasma EVs at diagnosis, as measured by flow cytometry, was found to be mainly of platelet origin, and these had procoagulant properties.[19] In our study, we utilized heparin as an anticoagulant, which can lead to platelet activation and release of platelet-derived microparticles.[20] We identified the platelet markers CD41 and CD61 in both plasma EVs and in the EVs directly isolated from B

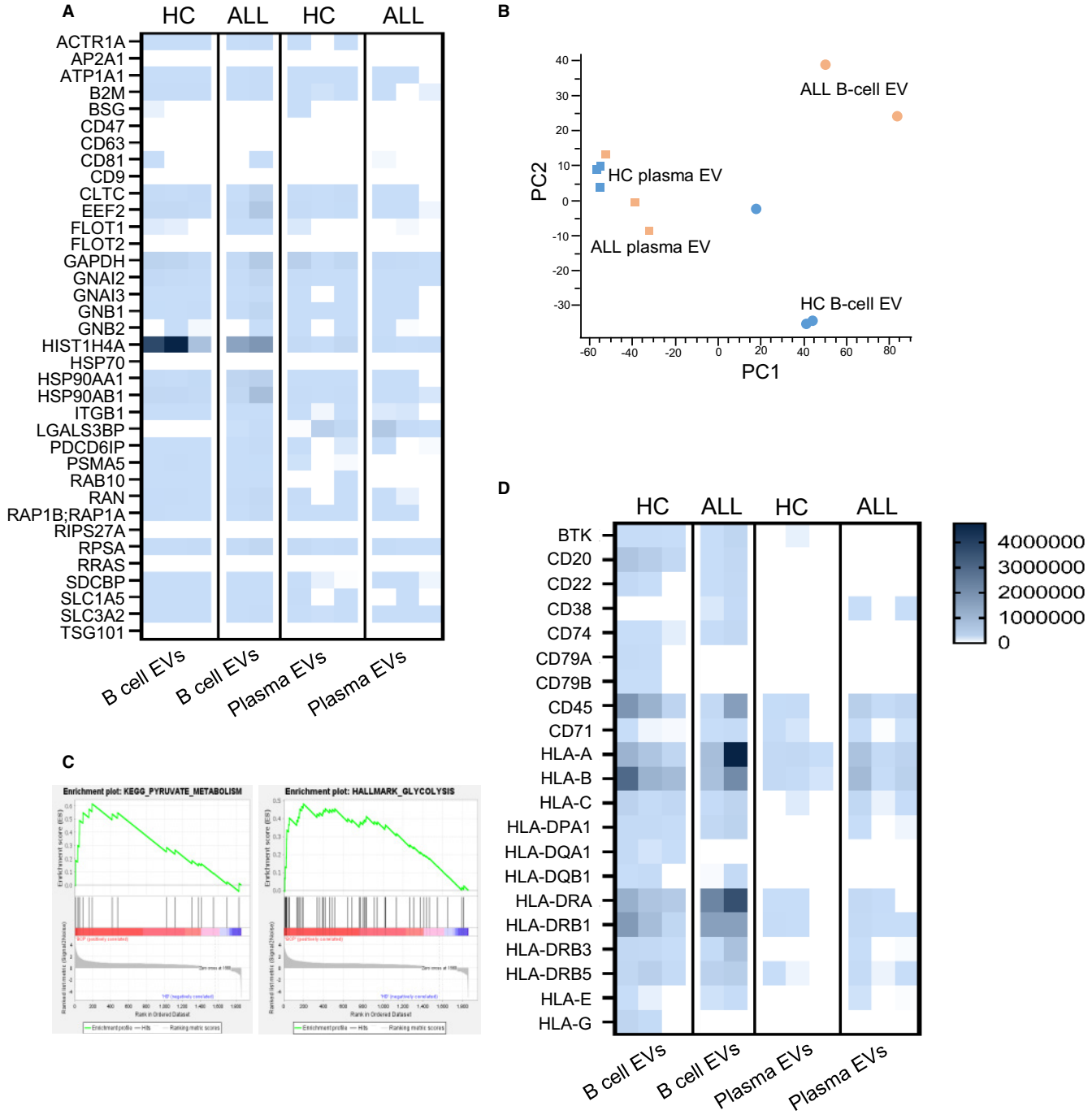

FIGURE 2 Comparative characterization of EVs derived from plasma and from B cells. EVs were isolated via precipitation followed by ultracentrifugation from purified B cells cultured for 48 h in serum-free medium from either healthy adult controls or from BCP-ALL patients, and from plasma from healthy paediatric controls or BCP-ALL patients. EVs were subjected to comparative LC–MS/MS analysis. (A) Heatmap analysis of EV-marker identifications in the four sample groups. Columns represent individual samples. (B) PCA analysis of the protein profiles obtained from the different samples. (C) Gene set enrichment analysis of the proteome identified in EVs derived from BCP-ALL blasts versus EVs derived from healthy control B cells. Hallmark_glycolysis, $P = .0307$. KEGG_pyruvate_metabolism, $P = .0133$. (D) Heatmap analysis of B-cell marker identifications in the four sample groups. Columns represent individual samples.

cells, but not to a higher extent than other immune markers, such as CD45, and the markers were equally distributed between patients and healthy donors. We therefore do not find it likely that the increased concentration of particles observed in patients stem from platelets. There was also no apparent enrichment of proteins associated with endothelial cells (selectins) or leukocytes (CD markers) between patients and controls. Pathway analysis, in contrast, highlighted a general enrichment of proteins related to glycolysis and pyruvate metabolism in plasma

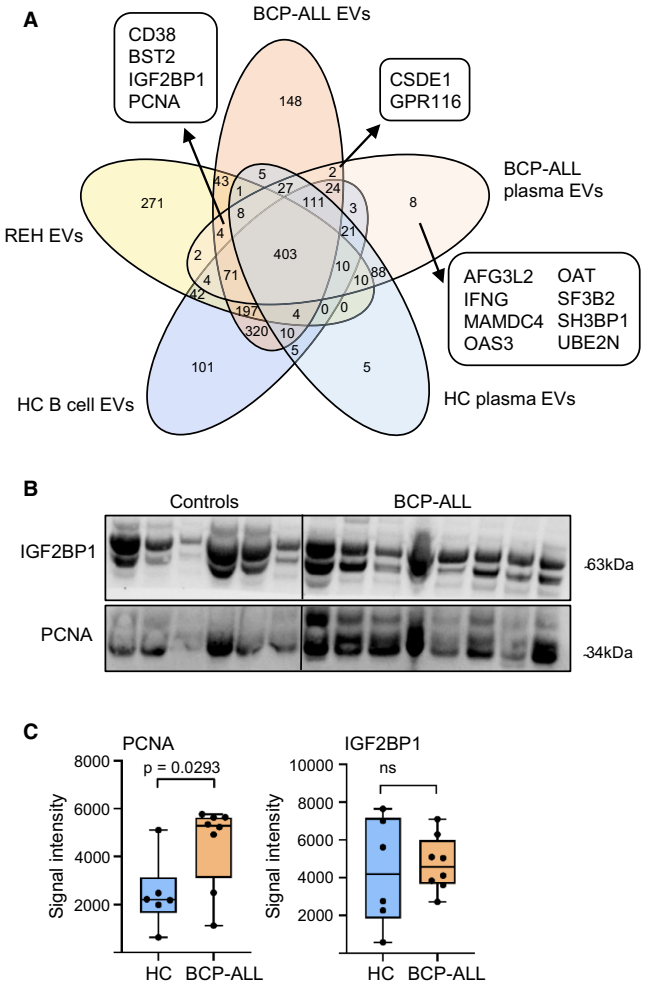

FIGURE 3 Identification of a core marker set in EVs from BCP-ALL. (A) 5-way Venn diagram analysis of overlapping protein signatures in EVs derived from healthy adult B cells, BCP-ALL blasts, REH cells and from plasma EVs of either healthy controls or BCP-ALL patients. (B) Western blot analysis of IGF2BP1 and PCNA in plasma EVs isolated from four patients and four healthy paediatric controls. (C) ImageJ analysis of signal intensity of bands in the Western blot analysis of eight patients and six healthy paediatric controls. Statistical significance was calculated using the non-parametrical Mann–Whitney test.

EVs from the patients. Potentially, if the EVs stem from internal sources in the cells, the enrichment of classifying surface markers may not be as distinct.

Immunophenotypic diagnostic panels for BCP-ALL includes among others CD19, CD10, and CD20 B-cell lineage markers as well as CD34, CD38, and IgM to distinguish specific sub-types of the disease.[21] While we detected B-cell markers such as CD20 in EVs derived directly from BCP-ALL blasts, we did not detect specific B-cell markers in EVs isolated from plasma. However, abundant expression of HLA class I and II was observed in EVs derived from both plasma and directly from B cells. CD38 was among the six markers identified specifically in EVs from BCP-ALL patients. CD38 is highly expressed by plasma cells, as well as by B-cell precursors.[22] BCP-ALL blasts reportedly express CD38 in a heterogenous manner, and used to distinguish subgroups of patients, with higher expression in patients with the favourable *ETV6-RUNX1* gene fusion and low expression in less favourable cytogenetics or in relapsing patients.[23] For the three patients tested in the proteomics analysis, two were *ETV6-RUNX1* and one was of hyperdiploid karyotype. Unfortunately, we were not able to experimentally test CD38 in EVs in a separate group of patients due to limitations of samples.

We confirmed an enrichment of PCNA but not IGF2BP1 in EVs from patients (mixed cytogenetic background) via Western blotting. Both PCNA and IGF2BP1 are reported to be overexpressed in BCP-ALL blasts.[24,25] PCNA is a nuclear protein upregulated in proliferating cells, such as leukaemic blasts.[24] IGF2BP1 is suggested to enhance tumour cell proliferation by sustaining elevated *MYC* expression,[26,27] and its presence in melanoma-derived EVs implicated in controlling their cargo and pro-metastatic abilities.[28,29] GPR116 and CSDE1 were uniquely identified in BCP-ALL EVs, but has to our knowledge not previously been directly implicated in the pathology of BCP-ALL. GPR116 is an adhesion type of G-protein-coupled receptors that is highly expressed by cancer stem cells,[30] and playing a role for invasion and metastasis of breast cancer cells.[31] CSDE1 is an RNA-binding protein regulating c-Fos, c-Myc, and Pten, and shown to promote an invasive phenotype of melanoma and colorectal cancer.[32]

A limitation to our study was the low amount of patient samples tested by proteomics, due to difficulties in obtaining viable B-cell cultures from BCP-ALL patients. Also, the sensitivity of the proteomic analysis was limited by the low concentration of EVs that served as input, due to quite extensive EV purification protocols. Despite these limitations, we have been able to perform a valuable proteomics comparison of EVs isolated from plasma with EVs derived directly from the blasts. The core protein marker set consisting of CD38, IGF2BP1, BST2, PCNA, CSDE1, or GPR116 are all logical markers that have either already been identified in BCP-ALL blasts or in EVs derived from other cancer forms. It would be interesting to test these markers in a larger cohort of patient EV samples to assess whether any of the markers are associated to risk status or different cytogenetics status.

In conclusion, we have in this study undertaken a proteomics approach to identify a core protein signature of BCP-ALL-derived EVs, which may be utilized to design future EV biomarker panels for acute leukaemia.

AUTHOR CONTRIBUTIONS

AU, TAN, YW, and MI conceptualized and designed the study; NEBS, MAL, MS, YW, and ES performed experiments;

NEBS, MAL, ES, YW, MI and TAN analysed and interpreted the data, NEBS and MI wrote the manuscript; all authors read, edited and approved the final manuscript.

ACKNOWLEDGMENTS

The authors thank the children, donors, and parents involved in this study. This work was supported by The South-Eastern Regional Health Authority under grant 2013068, UNIFOR-FRIMED, and Barnestiftelsen and Fondsstiftelsen at Oslo University Hospital. Mass spectrometry-based proteomic analyses were performed by the Proteomics Core Facility, Department of Immunology, University of Oslo/Oslo University Hospital, which is supported by the Core Facilities program of the South-Eastern Norway Regional Health Authority. This core facility is also a member of the National Network of Advanced Proteomics Infrastructure (NAPI), which is funded by the Research Council of Norway INFRASTRUKTUR-program (project number: 295910).

CONFLICT OF INTEREST STATEMENT

The authors declare no conflicts of interests.

DATA AVAILABILITY STATEMENT

The data that support the findings of this study are openly available in PRIDE at http://www.ebi.ac.uk/pride, reference number PXD044465.

ORCID

Marit Inngjerdingen https://orcid.org/0000-0001-8965-661X

REFERENCES

1. Toft N, Birgens H, Abrahamsson J, et al. Results of NOPHO ALL2008 treatment for patients aged 1–45 years with acute lymphoblastic leukemia. *Leukemia*. 2018;32(3):606-615.
2. Théry C, Witwer KW, Aikawa E, et al. Minimal information for studies of extracellular vesicles 2018 (MISEV2018): a position statement of the International Society for Extracellular Vesicles and update of the MISEV2014 guidelines. *J Extracell Vesicles*. 2018;7(1):1535750.
3. Valadi H, Ekström K, Bossios A, Sjöstrand M, Lee JJ, Lötvall JO. Exosome-mediated transfer of mRNAs and microRNAs is a novel mechanism of genetic exchange between cells. *Nat Cell Biol*. 2007;9(6):654-659.
4. Théry C. Exosomes: secreted vesicles and intercellular communications. F1000 biology reports. 2011;3.
5. Zomer A, Maynard C, Verweij FJ, et al. In vivo imaging reveals extracellular vesicle-mediated phenocopying of metastatic behavior. *Cell*. 2015;161(5):1046-1057.
6. Costa-Silva B, Aiello NM, Ocean AJ, et al. Pancreatic cancer exosomes initiate pre-metastatic niche formation in the liver. *Nat Cell Biol*. 2015;17(6):816-826.
7. Webber J, Yeung V, Clayton A. Extracellular vesicles as modulators of the cancer microenvironment. *Sem Cell Dev Biol*. 2015;40:27-34.
8. Hornick NI, Doron B, Abdelhamed S, et al. AML suppresses hematopoiesis by releasing exosomes that contain microRNAs targeting c-MYB. *Sci Signal*. 2016;9(444):ra88.
9. Kinjyo I, Bragin D, Grattan R, Winter SS, Wilson BS. Leukemia-derived exosomes and cytokines pave the way for entry into the brain. *J Leukoc Biol*. 2019;105(4):741-753.
10. Melo SA, Luecke LB, Kahlert C, et al. Glypican-1 identifies cancer exosomes and detects early pancreatic cancer. *Nature*. 2015;523(7559):177-182.
11. Trino S, Lamorte D, Caivano A, de Luca L, Sgambato A, Laurenzana I. Clinical relevance of extracellular vesicles in hematological neoplasms: from liquid biopsy to cell biopsy. *Leukemia*. 2021;35(3):661-678.
12. Tzoran I, Rebibo-Sabbah A, Brenner B, Aharon A. Disease dynamics in patients with acute myeloid leukemia: new biomarkers. *Exp Hematol*. 2015;43(11):936-943.
13. Szczepanski MJ, Szajnik M, Welsh A, Whiteside TL, Boyiadzis M. Blast-derived microvesicles in sera from patients with acute myeloid leukemia suppress natural killer cell function via membrane-associated transforming growth factor-β1. *Haematologica*. 2011;96(9):1302-1309.
14. Oksvold MP, Kullmann A, Forfang L, et al. Expression of B-cell surface antigens in subpopulations of exosomes released from B-cell lymphoma cells. *Clin Ther*. 2014;36(6):847-862. e841.
15. Heberle H, Meirelles GV, da Silva FR, Telles GP, Minghim R. InteractiVenn: a web-based tool for the analysis of sets through Venn diagrams. *BMC Bioinformatics*. 2015;16:1-7.
16. Kugeratski FG, Hodge K, Lilla S, et al. Quantitative proteomics identifies the core proteome of exosomes with syntenin-1 as the highest abundant protein and a putative universal biomarker. *Nat Cell Biol*. 2021;23(6):631-641.
17. Johnson SM, Dempsey C, Chadwick A, et al. Metabolic reprogramming of bone marrow stromal cells by leukemic extracellular vesicles in acute lymphoblastic leukemia. *Blood*. 2016;128(3):453-456.
18. Hong C-S, Muller L, Whiteside TL, Boyiadzis M. Plasma exosomes as markers of therapeutic response in patients with acute myeloid leukemia. *Front Immunol*. 2014;5:160.
19. Pluchart C, Barbe C, Poitevin G, Audonnet S, Nguyen P. A pilot study of procoagulant platelet extracellular vesicles and P-selectin increase during induction treatment in acute lymphoblastic leukaemia paediatric patients: two new biomarkers of thrombogenic risk? *J Thromb Thrombolysis*. 2021;51:711-719.
20. Witwer KW, Buzás EI, Bemis LT, et al. Standardization of sample collection, isolation and analysis methods in extracellular vesicle research. *J Extracell Vesicles*. 2013;2(1):20360.
21. Kulis J, Sędek Ł, Słota Ł, Perkowski B, Szczepański T. Commonly assessed markers in childhood BCP-ALL diagnostic panels and their association with genetic aberrations and outcome prediction. *Genes*. 2022;13(8):1374.
22. Lamkin T, Brooks J, Annett G, Roberts W, Weinberg K. Immunophenotypic differences between putative hematopoietic stem cells and childhood B-cell precursor acute lymphoblastic leukemia cells. *Leukemia*. 1994;8(11):1871-1878.
23. Chulián S, Martínez-Rubio Á, Pérez-García VM, et al. High-dimensional analysis of single-cell flow cytometry data predicts relapse in childhood acute lymphoblastic leukaemia. *Cancer*. 2020;13(1):17.

24. Keim D, Hailat N, Hodge D, Hanash SM. Proliferating cell nuclear antigen expression in childhood acute leukemia. *Blood*. 1990;76:985-990.
25. Nordlund J, Syvänen A-C. Epigenetics in pediatric acute lymphoblastic leukemia. *Semin Cancer Biol*. 2018;51:129-138.
26. Elcheva IA, Wood T, Chiarolanzio K, et al. RNA-binding protein IGF2BP1 maintains leukemia stem cell properties by regulating HOXB4, MYB, and ALDH1A1. *Leukemia*. 2020;34(5):1354-1363.
27. Weidensdorfer D, Stöhr N, Baude A, et al. Control of c-myc mRNA stability by IGF2BP1-associated cytoplasmic RNPs. *RNA*. 2009;15(1):104-115.
28. Ghoshal A, Rodrigues LC, Gowda CP, et al. Extracellular vesicle-dependent effect of RNA-binding protein IGF2BP1 on melanoma metastasis. *Oncogene*. 2019;38(21):4182-4196.
29. Wurth L, Papasaikas P, Olmeda D, et al. UNR/CSDE1 drives a post-transcriptional program to promote melanoma invasion and metastasis. *Cancer Cell*. 2016;30(5):694-707.
30. Bhat RR, Yadav P, Sahay D, et al. GPCRs profiling and identification of GPR110 as a potential new target in HER2+ breast cancer. *Breast Cancer Res Treat*. 2018;170:279-292.
31. Tang X, Jin R, Qu G, et al. GPR116, an adhesion G-protein–coupled receptor, promotes breast cancer metastasis via the Gαq-p63RhoGEF-rho GTPase pathway. *Cancer Res*. 2013;73(20):6206-6218.
32. Martinez-Useros J, Garcia-Carbonero N, Li W, et al. UNR/CSDE1 expression is critical to maintain invasive phenotype of colorectal cancer through regulation of c-MYC and epithelial-to-mesenchymal transition. *J Clin Med*. 2019;8(4):560.

SUPPORTING INFORMATION

Additional supporting information can be found online in the Supporting Information section at the end of this article.

How to cite this article: Saidu NEB, Aarsund M, Sørensen E, et al. Identifying a core protein signature of small extracellular vesicles derived from B-cell precursor acute lymphoblastic leukaemia. *Scand J Immunol*. 2023;00:e13341. doi:10.1111/sji.13341